ELSEVIER

Comput. Methods Appl. Mech. Engrg. 163 (1998) 323–341

Computer methods in applied mechanics and engineering

# Generalized Galerkin approximations of elastic waves with absorbing boundary conditions

A. Quarteroni[a,c,*], A. Tagliani[a], E. Zampieri[b]

[a]*Politecnico di Milano, Piazza L. da Vinci 32, 20133 Milano, Italy*
[b]*Università di Milano, via Saldini 50, 20133 Milano, Italy*
[c]*Centro di Ricerca, Sviluppo e Studi Superiori in Sardegna (CRS4), Cagliari, Italy*

Received 12 December 1997

**Abstract**

For the propagation of elastic waves in unbounded domains, absorbing boundary conditions (ABCs) at the fictitious numerical boundaries have been proposed. In this paper we focus on both first- and second-order ABCs in the framework of variational (weak) approximations, like those stemming from Galerkin method (or its variants) for finite element or spectral approximations [1]. In particular, we recover first order conditions as *natural* (or Neumann) conditions, whereas we propose a penalty residual method for the treatment of second order ABCs. The time discretization is based on implicit backward finite differences, whereas we use spectral Legendre collocation methods set in a variational form for the spatial discretization (treatment of finite element or spectral element approximations is completely similar). Numerical experiments exhibit that the present formulation of second-order ABCs improves the one based on first-order ABCs with regard to both the reduction of the total energy in the computational domain, and the Fourier spectrum of the displacement field at selected points of the elastic medium. A stability analysis is developed for the variational problem in the continuous case both for first- and second-order ABCs. A suitable treatment of ABCs at corners is also proposed. 

## 1. Introduction

Many geophysical or seismological engineering problems, including modeling of the Earth's crust and seismic exploration for gas and oil or soil-structure interaction, are problems in wave propagation requiring solution of the two- or three-dimensional wave equation. In obtaining a numerical solution, an essentially infinite domain is mapped onto a finite region with artificial boundaries. Provided that there are no external mechanism which cause reflection back into the domain, the artificial boundaries should simulate outward radiation of energy.

A customary approach for dealing with infinite media consists of introducing a fictitious boundary and setting non-reflecting conditions on it. These can be naturally formulated in the frequency domain, while they lead to non-local conditions (both in space and time) when included in space–time methods. For this reason, a number of local non-reflecting conditions have been proposed, based on the paraxial approximation of the wave equation [2] and characterized by the following features:

(i) they are exact for normal wave incidence, but their efficiency degrades for increasing $\theta$ and is minimal for parallel incidence.

(ii) A family of paraxial approximations with increasing efficiency exists, based on homogeneous linear combinations of space–time derivatives of the solution. A straightforward variational treatment is possible when the non-reflecting condition can be directly substituted in the traction term contained in the

* Corresponding author.

0045-7825/98/$19.00 
PII: S0045-7825(98)00022-X

variational formulation of wave equation. For this reason in this paper we take into account second-order ABCs, improving the first-order ones previously considered [3].

On the other hand, an increasing number of applications of the wave equations demand for highly accurate solution. To this purpose, higher-order methods, such as spectral collocation methods, enable one to achieve the expected accuracy using few grid points per minimum wavelength. Further, stability conditions of explicit time-marching schemes make the application of spectral methods very expensive when dealing with long time integration. To overcome this drawback several approaches have been considered, for instance, in the framework of domain decomposition methods [4–7].

In a previous paper [3], we proved that the time step $\Delta t$ of the implicit scheme is about ten times larger than the one obtained by adopting an explicit advancing scheme. Equivalently, the computational burden due to the implicit scheme is repayed by larger admissible $\Delta t$ values providing the same accuracy in the displacement Fourier spectrum of the explicit scheme. In the present paper we advocate second-order ABCs in a weak form (penalty residual method) and implicit advancing time scheme. The present formulation improves the one based on first-order ABCs as far the decrease of total energy in the computational domain is concerned, as well as the Fourier spectral ratio detected at some points of the elastic medium.

An outline of the paper is the following. In Section 2 we introduce the governing equations of the elasto-dynamic problem and recall both the sets of first- and second-order absorbing boundary conditions (ABC1 and ABC2 for brevity, respectively) proposed in [2,11] and developed later in [8]. We consider the variational formulation of the model problem. In this regard ABC1 can be enforced as natural (or *Neumann*) conditions, whereas we propose to fulfill ABC2 in weak from according to a penalty residual method. In Section 3 we analyze the stability of the continuous variational problem both for ABC1 and ABC2. In Section 4 we formulate the semi-discrete continuous-in-time problem. The spatial discretization is based either on finite element, or spectral collocation, or spectral element approximations. We also report the expressions of the stability estimates for the semidiscrete problems. In Section 5 we present several numerical results in order to show how ABC2 perform with respect to ABC1. The spatial discretization is based on Legendre–Gauss–Lobatto collocation methods set in variational (or weak) form, whereas we use implicit backward finite differences for the time discretization. We also show that the weak spectral approximation of ABC2 enforced according to the penalty residual method is similar to the discretization of natural boundary conditions. Finally, in Appendix A we propose a suitable treatment of absorbing boundary conditions at the corners of the domain.

## 2. Mathematical formulation of the problem

We consider a two-dimensional elastic medium, consisting of a solid, homogeneous, isotropic linear elastic material, occupying the finite region $\Omega \subset \mathbb{R}^2$. We denote with $\partial\Omega$ its boundary, with $\boldsymbol{n} = (n_1, n_2)$ the outward normal unit vector on $\partial\Omega$, and with $(0, T)$ the temporal interval, with $T$ real and positive.

The problem of interest here is the determination of the displacements $\boldsymbol{u} = (u_1, u_2)$, strain $\underline{\epsilon} = (\epsilon_{ij}(\boldsymbol{u}))$ and stress $\underline{\sigma} = (\sigma_{ij}(\boldsymbol{u}))$ fields produced in the body by the application of known distribution of external actions. Neglecting thermal effects, the latter might consist either of distributed loads $\boldsymbol{\Psi} = (\Psi_1, \Psi_2)$ over $\Gamma_L$, or displacements $\boldsymbol{\Phi} = (\Phi_1, \Phi 2)$ over $\Gamma_D$, or body forces $\boldsymbol{f} = (f_1, f_2)$ per unit volume in $\Omega$. The stress and strain tensor are related to the displacements by the Hooke's law

$$\sigma_{ij}(\boldsymbol{u}) = \lambda \operatorname{div} \boldsymbol{u}\, \delta_{ij} + \mu \epsilon_{ij}(\boldsymbol{u}) \quad i, j = 1, 2 \tag{2.1}$$

and by the equation of compatibility between strains and displacements, that reads

$$\epsilon_{ij}(\boldsymbol{u}) = \frac{1}{2}\left(\frac{\partial u_i}{\partial x_j} + \frac{\partial u_j}{\partial x_i}\right) \quad i, j = 1, 2 \tag{2.2}$$

where $\lambda$ and $\mu$ are the Lame's coefficients and $\delta_{ij}$ is the Kronecker index.

Through the principle of virtual works, the dynamic equilibrium equations for the medium are given by

$$\rho \frac{\partial^2 u_i}{\partial t^2} = \sum_{j=1}^{2} \frac{\partial \sigma_{ij}(\boldsymbol{u})}{\partial x_j} + f_i \equiv -(A\boldsymbol{u})_i + f_i \quad i = 1, 2 \quad \text{in } \Omega \times (0, T) \tag{2.3}$$

where $\rho > 0$ is the density of the material. The most commonly adopted solution strategy for the elastic problem is the one leading to the so-called displacement formulation of the stress analysis problem. The *equilibrium equations* (or *equations of momentum conservation*) are expressed first in terms of the strain components, by substituting the constitutive law (2.1) into (2.3) and then in terms of the displacements, by using the compatibility equations (2.2). The resulting set of equilibrium equations becomes (*Navier equations*)

$$\rho \frac{\partial^2 u_i}{\partial t^2} - \left[ \sum_{j=1}^{2} \left( \lambda + \frac{\mu}{2} \right) \frac{\partial^2 u_j}{\partial x_i \, \partial x_j} + \frac{\mu}{2} \sum_{j=1}^{2} \frac{\partial^2 u_i}{\partial x_j^2} \right] = f_i \quad i = 1, 2, \quad \text{in } \Omega \times (0, T) \tag{2.4}$$

with boundary conditions

$$\boldsymbol{u} = \boldsymbol{\Phi} \quad \text{on } \Gamma_{\mathrm{D}} \times (0, T) \quad (\textit{prescribed displacements}) \tag{2.5}$$

$$(\boldsymbol{B}\boldsymbol{u})_i \equiv \sum_{j=1}^{2} \sigma_{ij}(\boldsymbol{u}) n_j = \Psi_i \quad i = 1, 2 \quad \text{on } \Gamma_{\mathrm{L}} \times (0, T) \quad (\textit{prescribed loads}) \tag{2.6}$$

Both initial displacements $\boldsymbol{u}_0$ and velocities $\boldsymbol{u}_1$ need also to be specified in the present case:

$$\boldsymbol{u}(\boldsymbol{x}, 0) = \boldsymbol{u}_0(\boldsymbol{x}) \quad \boldsymbol{x} \in \Omega \tag{2.7}$$

$$\frac{\partial \boldsymbol{u}}{\partial t}(\boldsymbol{x}, 0) = \boldsymbol{u}_1(\boldsymbol{x}) \quad \boldsymbol{x} \in \Omega \tag{2.8}$$

To introduce the weak (or variational) formulation of (2.4)–(2.8), we need to define some functional spaces along with their norms and inner products that are used hereafter. In particular, we introduce the spaces

$$H^1(\Omega) = \{ v \in L^2(\Omega) : \nabla v \in [L^2(\Omega)]^2 \} \tag{2.9}$$

$$V(\Omega) = \{ \boldsymbol{v} \in [H^1(\Omega)]^2, \ \boldsymbol{v} = \boldsymbol{0} \text{ on } \Gamma_{\mathrm{D}} \} \tag{2.10}$$

where $L^2(\Omega)$ is the space of measurable functions in $\Omega$ whose square is integrable in $\Omega$. The inner products of $L^2(\Omega)$ and $H^1(\Omega)$ are given by

$$(u, v) \equiv \int_\Omega uv \, \mathrm{d}x_1 \, \mathrm{d}x_2 , \qquad (u, v)_{H^1(\Omega)} \equiv (u, v) + (\nabla u, \nabla v) = \int_\Omega (uv + \nabla u \cdot \nabla v) \, \mathrm{d}x_1 \, \mathrm{d}x_2$$

and the corresponding norms by

$$\|v\| = \sqrt{(v, v)} , \qquad \|v\|_{H^1(\Omega)} = \sqrt{(v, v)_{H^1(\Omega)}} \tag{2.11}$$

The weak formulation of problem (2.4)–(2.6) reads:
find $\boldsymbol{u} : (0, T) \to [H^1(\Omega)]^2$ such that, $\forall\, t \in (0, T)$, $\boldsymbol{u}(t) = \boldsymbol{\Phi}(t)$ on $\Gamma_{\mathrm{D}}$ and

$$\left( \rho \frac{\partial^2 \boldsymbol{u}}{\partial t^2}, \boldsymbol{v} \right) + a(\boldsymbol{u}, \boldsymbol{v}) = (\boldsymbol{f}, \boldsymbol{v}) + \langle \boldsymbol{\Psi}, \boldsymbol{v} \rangle_{\Gamma_{\mathrm{L}}} \quad \forall\, \boldsymbol{v} \in V(\Omega) \tag{2.12}$$

Here

$$(\boldsymbol{u}, \boldsymbol{v}) \equiv \sum_{i=1}^{2} (u_i, v_i) \tag{2.13}$$

$$\langle \boldsymbol{u}, \boldsymbol{v} \rangle_\Gamma \equiv \sum_{i=1}^{2} \int_\Gamma u_i v_i \, \mathrm{d}s , \qquad \|\boldsymbol{u}\|_\Gamma^2 \equiv \sum_{i=1}^{2} \|u_i\|_\Gamma^2 \equiv \sum_{i=1}^{2} \int_\Gamma u_i^2 \, \mathrm{d}s \tag{2.14}$$

where $\Gamma$ is a portion of the boundary $\partial\Omega$, e.g. $\Gamma = \Gamma_{\mathrm{L}}$.

Finally,

$$a(\boldsymbol{u}, \boldsymbol{v}) \equiv \int_\Omega \left( \lambda \operatorname{div} \boldsymbol{u} \operatorname{div} \boldsymbol{v} + \mu \sum_{ij=1}^{2} \epsilon_{ij}(\boldsymbol{u}) \epsilon_{ij}(\boldsymbol{v}) \right) \mathrm{d}x_1 \, \mathrm{d}x_2 \tag{2.15}$$

is a V-elliptic, continuous, symmetric bilinear form. We recall that these conditions guarantee that problem (2.12) admits a unique solution $\boldsymbol{u} \in L^\infty(0, T;\ [L^2(\Omega)]^2 \cap L^2(0, T;\ [H^1(\Omega)]^2)$ (e.g. [9,10]).

### 2.1. Absorbing boundary condition

In the simulation of wave propagation through an unbounded domain, it is a common practice to truncate the original domain into a finite domain. On artificial boundaries which are created by truncation, certain types of boundary conditions have to be imposed in order to eliminate (or to keep as low as possible) spurious wave reflections. Theoretically, one can find exact transmitting boundary conditions. However, such conditions are non-local neither in space nor in time: the resulting problems involve pseudodifferential operators, and thus the exact conditions are not useful for numerical computation.

The most popular set of ABCs were introduced by Clayton and Engquist [2] and Engquist and Majda [11,8]. The aim is to make the boundary transparent to outgoing and opaque to ingoing waves. This is achieved by means of paraxial approximations to the elastic wave equations, that are only valid for outgoing waves. Clayton and Engquist derived different kinds of absorbing boundary conditions. Their accuracy can be increased by taking higher-order paraxial approximations.

In this paper we draw our attention on both ABC1 and ABC2 proposed in [2,11,8]. In particular, the advantages of ABC2, compared to ABC1, is that they absorb energy over a wide range of incident angles. These families of ABCs depend on both the compressional and shear velocities, which can be expressed as functions of the Lame's parameters $\lambda$ and $\mu$ and of the density $\rho$:

$$\alpha = \sqrt{\frac{\lambda + \mu}{\rho}} \qquad \beta = \sqrt{\frac{\mu}{2\rho}} \tag{2.16}$$

We will refer to the rectangular domain $\Omega = [x_{1a}, x_{1b}] \times [x_{2a}, x_{2b}]$. Therefore, the boundary $\partial\Omega$ is given by sides parallel to the reference axes. We denote by $\Gamma_{AB}$ the artificial boundary where ABCs are enforced. The expression of the ABC1 is

$$\frac{1}{\beta}\frac{\partial u_1}{\partial t} + \frac{\partial u_1}{\partial \boldsymbol{n}} = 0\,, \qquad \frac{1}{\alpha}\frac{\partial u_2}{\partial t} + \frac{\partial u_2}{\partial \boldsymbol{n}} = 0 \tag{2.17}$$

and the corresponding variational formulation of the elastodynamic problem with ABC1 reads [3]: find $\boldsymbol{u} : (0, T) \to [H^1(\Omega)]^2$ such that, $\forall\, t \in (0, T)$, $\boldsymbol{u}(t) = \boldsymbol{\Phi}(t)$ on $\Gamma_D$ and

$$\left(\rho \frac{\partial^2 \boldsymbol{u}}{\partial t^2}, \boldsymbol{v}\right) + a(\boldsymbol{u}, \boldsymbol{v}) + \langle -B\boldsymbol{u}, \boldsymbol{v}\rangle_{\Gamma_{AB}} = (\boldsymbol{f}, \boldsymbol{v}) + \langle \boldsymbol{\Psi}, \boldsymbol{v}\rangle_{\Gamma_L} \quad \forall\, \boldsymbol{v} \in V(\Omega) \tag{2.18}$$

We notice that, since the boundary operator $B$ introduced in (2.6) involves first-order derivatives only, the set of ABC1 (2.17) can be enforced directly in (2.18) by inserting the partial derivatives $\partial u_i / \partial t$ into the term $\langle \cdot, \cdot \rangle_{\Gamma_{AB}}$ at the place of the normal derivatives $\partial u_i / \partial \boldsymbol{n}$. If we indicate with $\boldsymbol{s} = (n_2, -n_1)$ the *tangential* unit vector on $\partial\Omega$, then ABC2 read

$$C\boldsymbol{u} \equiv \boldsymbol{u}_{tn} + C_1\boldsymbol{u}_{tt} + C_2\boldsymbol{u}_{ts} + C_3\boldsymbol{u}_{ss} = \boldsymbol{0} \quad \text{on } \Gamma_{AB} \tag{2.19}$$

Matrices $C_i$, $i = 1, 2, 3$, are defined as follows:

*on horizontal sides*

$$C_1 = \begin{bmatrix} \frac{1}{\beta} & 0 \\ 0 & \frac{1}{\alpha} \end{bmatrix} \qquad C_2 = \begin{bmatrix} 0 & \frac{\alpha - \beta}{\beta} \\ \frac{\alpha - \beta}{\alpha} & 0 \end{bmatrix} \qquad C_3 = \begin{bmatrix} \frac{\beta - 2\alpha}{2} & 0 \\ 0 & \frac{\alpha - 2\beta}{2} \end{bmatrix}$$

*on vertical sides*

$$C_1 = \begin{bmatrix} \frac{1}{\alpha} & 0 \\ 0 & \frac{1}{\beta} \end{bmatrix} \quad C_2 = \begin{bmatrix} 0 & \frac{\beta-\alpha}{\alpha} \\ \frac{\beta-\alpha}{\beta} & 0 \end{bmatrix} \quad C_3 = \begin{bmatrix} \frac{\alpha-2\beta}{2} & 0 \\ 0 & \frac{\beta-2\alpha}{2} \end{bmatrix}$$

The formulation of the variational elastodynamic problem is the same as in (2.18). Nevertheless, the presence of second-order derivatives in the expression of $\boldsymbol{Cu}$ (2.19) makes it impossible the fulfillment of (2.19) by inserting them directly into the expression of $\boldsymbol{Bu}$ as we did instead for ABC1. Thus, we propose to enforce ABC2 (2.19) in a weak form, adding a new term to the previous expression.

Precisely, the new formulation (*penalty residual method*) writes:
find $\boldsymbol{u} : (0, T) \to [H^1(\Omega)]^2$ such that, $\forall t \in (0, Y)$, $\boldsymbol{u}(t) = \boldsymbol{\Phi}(t)$ on $\Gamma_D$ and

$$\left(\rho \frac{\partial^2 \boldsymbol{u}}{\partial t^2}, \boldsymbol{v}\right) + a(\boldsymbol{u}, \boldsymbol{v}) + \langle -\boldsymbol{Bu}, \boldsymbol{v}\rangle_{\Gamma_{AB}} + \langle \boldsymbol{Cu}, \boldsymbol{v}\rangle_{\Gamma_{AB}} = (f, \boldsymbol{v}) + \langle \boldsymbol{\psi}, \boldsymbol{v}\rangle_{\Gamma_L} \quad \forall \boldsymbol{v} \in V(\Omega) \tag{2.20}$$

## 3. Stability inequalities for absorbing boundary conditions

We investigate here the stability of the elastodynamic problems (2.18) and (2.20) in the case of mixed ABCs-displacement boundary conditions. Consequently $\Gamma_L = \emptyset$ and the term involving $\langle \cdot, \cdot \rangle_{\Gamma_L}$ is not present. For the sake of exposition, we assume ABCs to be prescribed only on the upper side, while displacement boundary conditions are assumed on the remaining sides of the boundary $\partial\Omega$. Then, $\Gamma_{AB} = \{x_2 = x_{2b}, x_{1a} < x_1 < x_{1b}\}$ (see Fig. 1). Moreover, for the simplicity of exposition we consider $\boldsymbol{\Phi} = 0$, $\rho = 1$ and homogeneous initial conditions, i.e. $\boldsymbol{u}_0 = \boldsymbol{0}$, $\boldsymbol{u}_1 = \boldsymbol{0}$.

### 3.1. First-order absorbing boundary conditions (ABC1)

We investigate here the stability of the variational problem in the case of mixed ABC1-displacement boundary conditions. We carry out our proof starting from the variational formulation (2.18). In particular, we recall that on the upper horizontal side the boundary operator $B$ takes the following form:

$$(\boldsymbol{Bu})_1 = \frac{\mu}{2}\left(\frac{\partial u_1}{\partial x_2} + \frac{\partial u_2}{\partial x_1}\right), \qquad (\boldsymbol{Bu})_2 = \lambda \frac{\partial u_1}{\partial x_1} + (\lambda + \mu)\frac{\partial u_2}{\partial x_2} \tag{3.1}$$

At each $t$ we choose the test function $\boldsymbol{v} = \partial \boldsymbol{u}/\partial t$, then integrate in time from $t = 0$ to $t = T$. We have

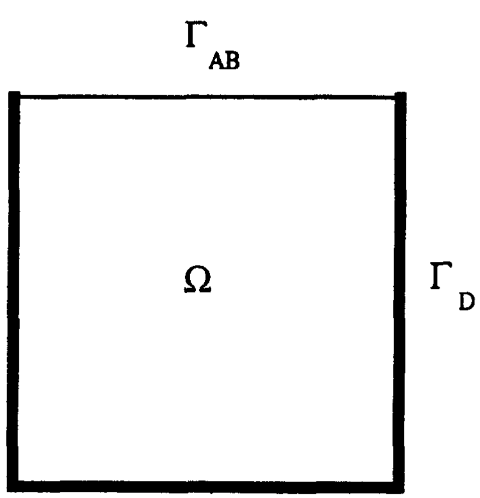


Fig. 1. Computational domain and boundary conditions.

$$\int_0^T \left(\frac{\partial^2 \boldsymbol{u}}{\partial t^2}, \frac{\partial \boldsymbol{u}}{\partial t}\right) \mathrm{d}t + \int_0^T a\left(\boldsymbol{u}, \frac{\partial \boldsymbol{u}}{\partial t}\right) \mathrm{d}t + \int_0^T \left\langle -B\boldsymbol{u}, \frac{\partial \boldsymbol{u}}{\partial t}\right\rangle_{\Gamma_{AB}} \mathrm{d}t = \int_0^T \left(\boldsymbol{f}, \frac{\partial \boldsymbol{u}}{\partial t}\right) \mathrm{d}t \tag{3.2}$$

Integrating in time the first and second integral and applying the Cauchy–Schwarz inequality to the right-hand side we obtain, respectively

$$\int_0^T \left(\frac{\partial^2 \boldsymbol{u}}{\partial t^2}, \frac{\partial \boldsymbol{u}}{\partial t}\right) \mathrm{d}t = \frac{1}{2} \left\| \frac{\partial \boldsymbol{u}}{\partial t}(T) \right\|^2 \tag{3.3}$$

$$\int_0^T a\left(\boldsymbol{u}, \frac{\partial \boldsymbol{u}}{\partial t}\right) \mathrm{d}t = \frac{1}{2} a(\boldsymbol{u}(T), \boldsymbol{u}(T)) \tag{3.4}$$

$$\int_0^T \left(\boldsymbol{f}, \frac{\partial \boldsymbol{u}}{\partial t}\right) \mathrm{d}t \leq \frac{1}{2} \int_0^T \left( \|\boldsymbol{f}\|^2 + \left\| \frac{\partial \boldsymbol{u}}{\partial t} \right\|^2 \right) \mathrm{d}t \tag{3.5}$$

As far as it concerns the third integral in (3.2), if we insert (2.17) into the boundary operator $B$ (3.1), we have

$$\begin{aligned}
\int_0^T \left\langle -B\boldsymbol{u}, \frac{\partial \boldsymbol{u}}{\partial t}\right\rangle_{\Gamma_{AB}} &\equiv \int_0^T \left( \sum_{i=1}^{2} \int_{\Gamma_{AB}} (-B\boldsymbol{u})_i \frac{\partial u_i}{\partial t} \mathrm{d}x_1 \right) \mathrm{d}t \\
&= \int_0^T \int_{\Gamma_{AB}} \left( \frac{\mu}{2} \frac{1}{\beta} \frac{\partial u_1}{\partial t} - \frac{\mu}{2} \frac{\partial u_2}{\partial x_1} \right) \frac{\partial u_1}{\partial t} \mathrm{d}x_1\, \mathrm{d}t + \int_0^T \int_{\Gamma_{AB}} \left( -\lambda \frac{\partial u_1}{\partial x_1} + \frac{1}{\alpha}(\lambda + \mu) \frac{\partial u_2}{\partial t} \right) \frac{\partial u_2}{\partial t} \mathrm{d}x_1\, \mathrm{d}t \\
&= \beta \int_0^T \left\| \frac{\partial u_1}{\partial t} \right\|^2_{\Gamma_{AB}} \mathrm{d}t + \alpha \int_0^T \left\| \frac{\partial u_2}{\partial t} \right\|^2_{\Gamma_{AB}} \mathrm{d}t - \int_0^T \int_{\Gamma_{AB}} \left( \frac{\mu}{2} \frac{\partial u_2}{\partial x_1} \frac{\partial u_1}{\partial t} + \lambda \frac{\partial u_1}{\partial x_1} \frac{\partial u_2}{\partial t} \right) \mathrm{d}x_1\, \mathrm{d}t
\end{aligned} \tag{3.6}$$

The first and second integrals in the last expression provide an additional positive contribution to the left-hand side of (3.2). Furthermore, if we apply the Cauchy–Schwarz inequality to the third integral in (3.6) we obtain

$$-\frac{\mu}{2} \int_0^T \int_{\Gamma_{AB}} \frac{\partial u_2}{\partial x_1} \frac{\partial u_1}{\partial t} \mathrm{d}x_1\, \mathrm{d}t \leq \frac{1}{2} \frac{\mu}{2} \int_0^T \left( \left\| \frac{\partial u_2}{\partial x_1} \right\|^2_{\Gamma_{AB}} + \left\| \frac{\partial u_1}{\partial t} \right\|^2_{\Gamma_{AB}} \right) \mathrm{d}t \tag{3.7}$$

$$-\lambda \int_0^T \int_{\Gamma_{AB}} \frac{\partial u_2}{\partial x_1} \frac{\partial u_2}{\partial t} \mathrm{d}x_1\, \mathrm{d}t \leq \frac{1}{2} \lambda \int_0^T \left( \left\| \frac{\partial u_1}{\partial x_1} \right\|^2_{\Gamma_{AB}} + \left\| \frac{\partial u_2}{\partial t} \right\|^2_{\Gamma_{AB}} \right) \mathrm{d}t \tag{3.8}$$

If we set

$$\gamma = \max\left\{ \frac{\mu}{4}, \frac{\lambda}{2} \right\}$$

the sum of the right-hand sides of (3.7) and (3.8) can be bounded by

$$\gamma \int_0^T \|\boldsymbol{u}\|^2_{H^1(\Omega)} \mathrm{d}t + \gamma \int_0^T \left\| \frac{\partial \boldsymbol{u}}{\partial t} \right\|^2 \mathrm{d}t \tag{3.9}$$

Finally, if we summarize (3.3)–(3.9) we obtain

$$\frac{1}{2} \left( \left\| \frac{\partial \boldsymbol{u}}{\partial t}(T) \right\|^2 + a(\boldsymbol{u}(T), \boldsymbol{u}(T)) \right) \leq \int_0^T \left[ (1+\gamma) \left( \left\| \frac{\partial \boldsymbol{u}}{\partial t} \right\|^2 + \|\boldsymbol{u}\|^2_{H^1(\Omega)} \right) + \|\boldsymbol{f}\|^2 \right] \mathrm{d}t \tag{3.10}$$

Setting

$$|||\boldsymbol{u}|||^2 = \frac{1}{2} \left( \left\| \frac{\partial \boldsymbol{u}}{\partial t} \right\|^2 + a(\boldsymbol{u}, \boldsymbol{u}) \right) \tag{3.11}$$

and using the coercivity of the bilinear form $a(\cdot, \cdot)$ [9,10]:

$$\exists\, \gamma_1 > 0 \text{ such that } a(\boldsymbol{u}, \boldsymbol{u}) \geq \gamma_1 \|\boldsymbol{u}\|^2_{H^1(\Omega)}, \quad \forall\, \boldsymbol{u} \in [H^1(\Omega)]^2$$

the stability estimate follows from Gronwall's lemma. Indeed, we obtain

$$\|u(T)\|^2 \leq \int_0^T \|f(s)\|^2 \, e^{C(t-s)} \, ds \tag{3.12}$$

for a suitable positive constant $C$ depending on $\gamma$ and $\gamma_1$.

### 3.2. Second-order absorbing boundary conditions (ABC2)

We investigate now the stability of the elasto-dynamic problem in the case of mixed ABC2-displacement boundary conditions. We carry out our proof starting from the variational formulation (2.20). According to (2.19) the ABC2 on the upper horizontal side take the following form (up to a couple of constants $\beta$ and $\alpha$):

$$\beta \frac{\partial^2 u_1}{\partial t\, \partial x_2} + \frac{\partial^2 u_1}{\partial t^2} + (\alpha - \beta) \frac{\partial^2 u_2}{\partial t\, \partial x_1} + \beta \frac{\beta - 2\alpha}{2} \frac{\partial^2 u_1}{\partial x_1^2} = 0 \tag{3.13}$$

$$\alpha \frac{\partial^2 u_2}{\partial t\, \partial x_2} + \frac{\partial^2 u_2}{\partial t^2} + (\alpha - \beta) \frac{\partial^2 u_1}{\partial t\, \partial x_1} + \alpha \frac{\alpha - 2\beta}{2} \frac{\partial^2 u_2}{\partial x_1^2} = 0 \tag{3.14}$$

At any $t > 0$ we choose as test function $\boldsymbol{v} = \partial \boldsymbol{u}(t)/\partial t$ then we integrate from $t = 0$ to $t = T$. We have

$$\int_0^T \left( \frac{\partial^2 \boldsymbol{u}}{\partial t^2}, \frac{\partial \boldsymbol{u}}{\partial t} \right) dt + \int_0^T a\left( \boldsymbol{u}, \frac{\partial \boldsymbol{u}}{\partial t} \right) dt + \int_0^T \left\langle -B\boldsymbol{u}, \frac{\partial \boldsymbol{u}}{\partial t} \right\rangle_{\Gamma_{AB}} dt + \int_0^T \left\langle C\boldsymbol{u}, \frac{\partial \boldsymbol{u}}{\partial t} \right\rangle_{\Gamma_{AB}} dt = \int_0^T \left( f, \frac{\partial \boldsymbol{u}}{\partial t} \right) dt \tag{3.15}$$

The first and second integral can be handled as in ABC1. Precisely, we have

$$\int_0^T \left( \frac{\partial^2 \boldsymbol{u}}{\partial t^2}, \frac{\partial \boldsymbol{u}}{\partial t} \right) dt = \frac{1}{2} \left\| \frac{\partial \boldsymbol{u}(T)}{\partial t} \right\|^2 \tag{3.16}$$

$$\int_0^T a\left( \boldsymbol{u}, \frac{\partial \boldsymbol{u}}{\partial t} \right) dt = \frac{1}{2} a(\boldsymbol{u}(T), \boldsymbol{u}(T)) \tag{3.17}$$

Then, we examine the terms involving the boundary operators $B$ and $C$.

From (3.1) it follows:

$$\begin{aligned} \int_0^T \left\langle -B\boldsymbol{u}, \frac{\partial \boldsymbol{u}}{\partial t} \right\rangle_{\Gamma_{AB}} dt &= \int_0^T \left( \sum_{i=1}^2 \int_{\Gamma_{AB}} (-B\boldsymbol{u})_i \frac{\partial u_i}{\partial t} \, dx_1 \right) dt \\ &= -\int_0^T \int_{\Gamma_{AB}} \left[ \frac{\mu}{2} \left( \frac{\partial u_1}{\partial x_2} + \frac{\partial u_2}{\partial x_1} \right) \frac{\partial u_1}{\partial t} + \left( \lambda \frac{\partial u_1}{\partial x_1} + (\lambda + \mu) \frac{\partial u_2}{\partial x_2} \right) \frac{\partial u_2}{\partial t} \right] dx_1 \, dt \end{aligned} \tag{3.18}$$

Finally, we consider the terms involving the boundary operator $C$, whose expression is reported in (3.13) and (3.14). They read

$$\begin{aligned} \int_0^T \left\langle C\boldsymbol{u}, \frac{\partial \boldsymbol{u}}{\partial t} \right\rangle_{\Gamma_{AB}} dt &= \int_0^T \left( \sum_{i=1}^2 \int_{\Gamma_{AB}} (C\boldsymbol{u})_i \frac{\partial u_i}{\partial t} \, dx_1 \right) dt \\ &= \int_0^T \int_{\Gamma_{AB}} \left( \beta \frac{\partial^2 u_1}{\partial t\, \partial x_2} + \frac{\partial^2 u_1}{\partial t^2} + (\alpha - \beta) \frac{\partial^2 u_2}{\partial t\, \partial x_1} + \beta \frac{\beta - 2\alpha}{2} \frac{\partial^2 u_1}{\partial x_1^2} \right) \frac{\partial u_1}{\partial t} \, dx_1 \, dt \\ &\quad + \int_0^T \int_{\Gamma_{AB}} \left( \alpha \frac{\partial^2 u_2}{\partial t\, \partial x_2} + \frac{\partial^2 u_2}{\partial t^2} + (\alpha - \beta) \frac{\partial^2 u_1}{\partial t\, \partial x_1} + \alpha \frac{\alpha - 2\alpha}{2} \frac{\partial^2 u_2}{\partial x_1^2} \right) \frac{\partial u_2}{\partial t} \, dx_1 \, dt \end{aligned} \tag{3.19}$$

Let us consider each term separately. The two terms involving second derivatives with respect to $t$ can be written as follows:

$$\int_0^T \int_{\Gamma_{AB}} \frac{\partial^2 u_1}{\partial t^2} \frac{\partial u_1}{\partial t} \, dx_1 \, dt = \frac{1}{2} \left\| \frac{\partial u_1}{\partial t}(T) \right\|_{\Gamma_{AB}}^2 \tag{3.20}$$

$$\int_0^T \int_{\Gamma_{AB}} \frac{\partial^2 u_2}{\partial t^2} \frac{\partial u_2}{\partial t} \, dx_1 \, dt = \frac{1}{2} \left\| \frac{\partial u_2}{\partial t}(T) \right\|^2_{\Gamma_{AB}} \tag{3.21}$$

Summing up we obtain

$$\int_0^T \int_{\Gamma_{AB}} \frac{\partial^2 u_1}{\partial t^2} \frac{\partial u_1}{\partial t} \, dx_1 \, dt + \int_0^T \int_{\Gamma_{AB}} \frac{\partial^2 u_2}{\partial t^2} \frac{\partial u_2}{\partial t} \, dx_1 \, dt = \frac{1}{2} \left\| \frac{\partial \boldsymbol{u}}{\partial t}(T) \right\|^2_{\Gamma_{AB}} \tag{3.22}$$

which gives a positive contribution to the left-hand side of (3.15).

Next we consider the terms involving the mixed derivatives with respect to $t$ and to the tangential direction $x_1$. Using integration by parts we have

$$\begin{aligned}
&(\alpha - \beta) \int_0^T \int_{\Gamma_{AB}} \left( \frac{\partial^2 u_2}{\partial t \, \partial x_1} \frac{\partial u_1}{\partial t} + \frac{\partial^2 u_1}{\partial t \, \partial x_1} \frac{\partial u_2}{\partial t} \right) dx_1 \, dt \\
&= (\alpha - \beta) \int_0^T \left( \int_{\Gamma_{AB}} \frac{\partial^2 u_2}{\partial t \, \partial x_1} \frac{\partial u_1}{\partial t} \, dx_1 + \left[ \frac{\partial u_1}{\partial t} \frac{\partial u_2}{\partial t} \right] \Big|_{\partial \Gamma_{AB}} - \int_{\Gamma_{AB}} \frac{\partial u_1}{\partial t} \frac{\partial^2 u_2}{\partial t \, \partial x_1} \, dx_1 \right) dt \\
&= (\alpha - \beta) \int_0^T \left[ \left( \frac{\partial u_1}{\partial t} \frac{\partial u_2}{\partial t} \right)(x_{1_b}) - \left( \frac{\partial u_1}{\partial t} \frac{\partial u_2}{\partial t} \right)(x_{1_a}) \right] dt
\end{aligned} \tag{3.23}$$

Let us set

$$\eta_1 = \beta \frac{\beta - 2\alpha}{2} \qquad \eta_2 = \alpha \frac{\alpha - 2\beta}{2} \tag{3.24}$$

The last two terms in (3.19) containing second derivatives with respect to the tangential direction $x_1$ give

$$\begin{aligned}
&\int_0^T \int_{\Gamma_{AB}} \left( \beta \frac{\beta - 2\alpha}{2} \frac{\partial^2 u_1}{\partial x_1^2} \frac{\partial u_1}{\partial t} + \alpha \frac{\alpha - 2\beta}{2} \frac{\partial^2 u_2}{\partial x_1^2} \frac{\partial u_2}{\partial t} \right) dx_1 \, dt \\
&= \eta_1 \int_0^T \left( \left[ \frac{\partial u_1}{\partial x_1} \frac{\partial u_1}{\partial t} \right] \Big|_{\partial \Gamma_{AB}} - \int_{\Gamma_{AB}} \frac{\partial u_1}{\partial x_1} \frac{\partial^2 u_1}{\partial t \, \partial x_1} \, dx_1 \right) dt \\
&\quad + \eta_2 \int_0^T \left( \left[ \frac{\partial u_2}{\partial x_1} \frac{\partial u_2}{\partial t} \right] \Big|_{\partial \Gamma_{AB}} - \int_{\Gamma_{AB}} \frac{\partial u_2}{\partial x_1} \frac{\partial^2 u_2}{\partial t \, \partial x_1} \, dx_1 \right) dt
\end{aligned} \tag{3.25}$$

We note that the quantities within square brackets in (3.25) vanish on $\partial \Gamma_{AB}$, since we assume $\boldsymbol{u} = \boldsymbol{0}$ on $\partial \Omega \backslash \Gamma_{AB}$, $\forall t \in [0, T]$. Then, since $\boldsymbol{u} = \boldsymbol{0}$ and $\partial \boldsymbol{u} / \partial t = \boldsymbol{0}$ at the time $t = 0$, we obtain

$$\begin{aligned}
&\int_0^T \int_{\Gamma_{AB}} \left( \beta \frac{\beta - 2\alpha}{2} \frac{\partial^2 u_1}{\partial x_1^2} \frac{\partial u_1}{\partial t} + \alpha \frac{\alpha - 2\beta}{2} \frac{\partial^2 u_2}{\partial x_1^2} \frac{\partial u_2}{\partial t} \right) dx_1 \, dt \\
&= -\eta_1 \int_0^T \int_{\Gamma_{AB}} \frac{\partial u_1}{\partial x_1} \frac{\partial^2 u_1}{\partial t \, \partial x_1} \, dx_1 \, dt - \eta_2 \int_0^T \int_{\Gamma_{AB}} \frac{\partial u_2}{\partial x_1} \frac{\partial^2 u_2}{\partial t \, \partial x_1} \, dx_1 \, dt \\
&= -\frac{1}{2} \eta_1 \left\| \frac{\partial u_1}{\partial x_1}(T) \right\|^2_{\Gamma_{AB}} - \frac{1}{2} \eta_2 \left\| \frac{\partial u_2}{\partial x_1}(T) \right\|^2_{\Gamma_{AB}}
\end{aligned} \tag{3.26}$$

If we confine ourselves to the case

$$\eta_1 < 0 \,, \qquad \eta_2 < 0$$

and consider the physical constraint $\beta < \alpha$, then

$$1 < \frac{\alpha}{\beta} < 2 \,. \tag{3.27}$$

Therefore, (3.25) provides an additional positive contribution to the left-hand side of (3.19). In conclusion (3.15) is equivalent to

$$\frac{1}{2}\left(\left\|\frac{\partial \boldsymbol{u}}{\partial t}(T)\right\|^2 + a(\boldsymbol{u}(T),\boldsymbol{u}(T)) + \left\|\frac{\partial \boldsymbol{u}}{\partial t}(T)\right\|^2_{\Gamma_{AB}} - \eta_1\left\|\frac{\partial u_1}{\partial x_1}(T)\right\|^2_{\Gamma_{AB}} - \eta_2\left\|\frac{\partial u_2}{\partial x_1}(T)\right\|^2_{\Gamma_{AB}}\right)$$
$$= \int_0^T \left(f, \frac{\partial \boldsymbol{u}}{\partial t}\right) \mathrm{d}t + \int_0^T \int_{\Gamma_{AB}} \left[\frac{\mu}{2}\left(\frac{\partial u_1}{\partial x_2} + \frac{\partial u_2}{\partial x_1}\right)\frac{\partial u_1}{\partial t} + \left(\lambda\frac{\partial u_1}{\partial x_1} + (\lambda+\mu)\frac{\partial u_2}{\partial x_2}\right)\frac{\partial u_2}{\partial t}\right] \mathrm{d}x_1\, \mathrm{d}t$$
$$- \int_0^T \int_{\Gamma_{AB}} \left(\beta\frac{\partial^2 u_1}{\partial t\,\partial x_2}\frac{\partial u_1}{\partial t} + \alpha\frac{\partial^2 u_2}{\partial t\,\partial x_2}\frac{\partial u_2}{\partial t}\right) \mathrm{d}x_1\, \mathrm{d}t$$
$$- (\alpha-\beta)\int_0^T \left[\left(\frac{\partial u_1}{\partial t}\frac{\partial u_2}{\partial t}\right)(x_{1b}) - \left(\frac{\partial u_1}{\partial t}\frac{\partial u_2}{\partial t}\right)(x_{1a})\right] \mathrm{d}t \tag{3.28}$$

Finally, using (3.11) we can draw the following energy inequality:

$$|\!|\!|\boldsymbol{u}(T)|\!|\!|^2 \leq \int_0^T \left(f, \frac{\partial \boldsymbol{u}}{\partial t}\right) \mathrm{d}t + \int_0^T \int_{\Gamma_{AB}} \left[\frac{\mu}{2}\left(\frac{\partial u_1}{\partial x_2} + \frac{\partial u_2}{\partial x_1}\right)\frac{\partial u_1}{\partial t} + \left(\lambda\frac{\partial u_1}{\partial x_1} + (\lambda+\mu)\frac{\partial u_2}{\partial x_2}\right)\frac{\partial u_2}{\partial t}\right] \mathrm{d}x_1\, \mathrm{d}t$$
$$- \int_0^T \int_{\Gamma_{AB}} \left(\beta\frac{\partial^2 u_1}{\partial t\,\partial x_2}\frac{\partial u_1}{\partial t} + \alpha\frac{\partial^2 u_2}{\partial t\,\partial x_2}\frac{\partial u_2}{\partial t}\right) \mathrm{d}x_1\, \mathrm{d}t$$
$$- (\alpha-\beta)\int_0^T \left[\left(\frac{\partial u_1}{\partial t}\frac{\partial u_2}{\partial t}\right)(x_{1b}) - \left(\frac{\partial u_1}{\partial t}\frac{\partial u_2}{\partial t}\right)(x_{1a})\right] \mathrm{d}t \tag{3.29}$$

In Section 4 we will discuss the discrete counterpart of the above inequalities and in Section 5.2 we will present some numerical examples in the framework of spectral collocation methods.

*REMARK.* Note that the constraint (3.27) on $\alpha$ and $\beta$ is not too restrictive, as it is satisfied by a wide range of rocks and metals [12]. In [13] and [14] new transparent formulations were proposed that are stable over a wider range of the parameters with respect to that of [2].

## 4. The semidiscrete continuous-in-time problem

In this section we discuss the numerical counterpart of the variational formulations (2.18) and (2.20), as well as of the stability inequalities obtained in Section 3 for the continuous variational elastodynamic problems. In order to obtain a numerical approximation to these problems we address first the discretization of the space variable $\boldsymbol{x} = (x_1, x_2)$ only.

If we consider finite element approximations, or more generally any Galerkin method, we must replace the functional space $[H^1(\Omega)]^2$ with a finite dimensional subspace $X_h(\Omega)$, $V(\Omega)$ with a finite dimensional space $V_h(\Omega)$ and the solution $\boldsymbol{u}$ with the semidiscrete continuous-in-time discrete solution, i.e. $\boldsymbol{u}_h(t)$. Then, the partial derivatives with respect to the spatial variables $x_1$ and $x_2$ can be properly approximated through standard techniques according to the choice of the discrete functional space. Finally, the integrals involving the source terms $\boldsymbol{f}$ and $\boldsymbol{\Psi}$ can be computed via Gaussian quadrature rules. For details, we refer to [15,17]. Therefore, the Galerkin approximation of (2.18) reads:

find $\boldsymbol{u}_h : (0,T) \to X_h(\Omega)$ such that, $\forall\, t \in (0,T)$, $\boldsymbol{u}_h(t) = \boldsymbol{\Phi}_h(t)$ on $\Gamma_D$ and

$$\left(\rho\frac{\partial^2 \boldsymbol{u}_h}{\partial t^2}, \boldsymbol{v}_h\right) + a(\boldsymbol{u}_h, \boldsymbol{v}_h) + \langle -\boldsymbol{B}\boldsymbol{u}_h, \boldsymbol{v}_h\rangle_{\Gamma_{AB}} = (\boldsymbol{f}, \boldsymbol{v}_h) + \langle \boldsymbol{\Psi}, \boldsymbol{v}_h\rangle_{\Gamma_L} \quad \forall\, \boldsymbol{v}_h \in V_h(\Omega) \tag{4.1}$$

Similarly, the Galerkin approximation of (2.20) is

find $\boldsymbol{u}_h : (0,T) \to X_h(\Omega)$ such that, $\forall\, t \in (0,T)$, $\boldsymbol{u}_h(t) = \boldsymbol{\Phi}_h(t)$ on $\Gamma_D$ and

$$\left(\rho\frac{\partial^2 \boldsymbol{u}_h}{\partial t^2}, \boldsymbol{v}_h\right) + a(\boldsymbol{u}_h, \boldsymbol{v}_h) + \langle -\boldsymbol{B}\boldsymbol{u}_h, \boldsymbol{v}_h\rangle_{\Gamma_{AB}} + \langle \boldsymbol{C}\boldsymbol{u}_h, \boldsymbol{v}_h\rangle_{\Gamma_{AB}} = (\boldsymbol{f}, \boldsymbol{v}_h) + \langle \boldsymbol{\Psi}, \boldsymbol{v}_h\rangle_{\Gamma_L} \quad \forall\, \boldsymbol{v}_h \in V_h(\Omega) \tag{4.2}$$

In (4.1) and (4.2), for each $t > 0$ $\boldsymbol{\Phi}_h(t)$ denotes a suitable discrete approximation of $\boldsymbol{\Phi}(t)$. Then, with regard to the stability estimates obtained in Section 3, for the case of ABC1 we can obtain

$$\|\boldsymbol{u}_h(T)\|^2 \le \int_0^T \|\boldsymbol{f}(s)\|^2 e^{C(t-s)}\, ds \tag{4.3}$$

whereas for ABC2 we obtain

$$\begin{aligned}\|\boldsymbol{u}_h(T)\|^2 \le & \int_0^T \left(\boldsymbol{f}, \frac{\partial \boldsymbol{u}_h}{\partial t}\right) dt \\ & + \int_0^T \int_{\Gamma_{AB}} \left[\frac{\mu}{2}\left(\frac{\partial u_{1,h}}{\partial x_2} + \frac{\partial u_{2,h}}{\partial x_1}\right)\frac{\partial u_{1,h}}{\partial t} + \left(\lambda \frac{\partial u_{1,h}}{\partial x_1} + (\lambda+\mu)\frac{\partial u_{2,h}}{\partial x_2}\right)\frac{\partial u_{2,h}}{\partial t}\right] dx_1\, dt \\ & - \int_0^T \int_{\Gamma_{AB}} \left(\beta \frac{\partial^2 u_{1,h}}{\partial t\, \partial x_2}\frac{\partial u_{1,h}}{\partial t} + \alpha \frac{\partial^2 u_{2,h}}{\partial t\, \partial x_2}\frac{\partial u_{2,h}}{\partial t}\right) dx_1\, dt \\ & - (\alpha - \beta)\int_0^T \left[\left(\frac{\partial u_{1,h}}{\partial t}\frac{\partial u_{2,h}}{\partial t}\right)(x_{1b}) - \left(\frac{\partial u_{1,h}}{\partial t}\frac{\partial u_{2,h}}{\partial t}\right)(x_{1a})\right] dt \end{aligned} \tag{4.4}$$

If we consider now the spectral weak collocation methods based on Legendre–Gauss–Lobatto points (LGL for brevity), or similarly any pseudo-Galerkin method, we must replace $\boldsymbol{u}(t)$ with $\boldsymbol{u}_N(t)$ where $\boldsymbol{u}_N(t) = (u_{1,N}(t), u_{2,N}(t))$ is a pair of algebraic polynomials of degree $\le N$ in each variable. Then, $\boldsymbol{u}_N(t) \in [\mathbb{P}_N(\Omega)]^2$, being $\Omega$ a rectangular domain. In this case the derivatives of $\boldsymbol{u}_N$ with respect to $x_1$ and $x_2$ can be computed exactly through the pseudospectral differentiation matrices (e.g. [15]). Finally, the norms, the inner products and the integrals over $\Gamma_{AB}$ and over $\Omega$ must be replaced with LGL quadrature formulas using, for each $t$, the values of the spectral solution $\boldsymbol{u}_N$ at the collocation points.

Precisely:

$$a(\boldsymbol{u}, \boldsymbol{v}) \approx a_N(\boldsymbol{u}_N, \boldsymbol{v}_N)$$
$$(\boldsymbol{u}, \boldsymbol{v}) \approx (\boldsymbol{u}_N, \boldsymbol{v}_N)_N$$
$$\langle \boldsymbol{u}, \boldsymbol{v}\rangle_\Gamma \approx \langle \boldsymbol{u}_N, \boldsymbol{v}_N\rangle_{\Gamma,N}$$

with $\Gamma = \Gamma_L$ or $\Gamma = \Gamma_{AB}$. The discrete norms are defined accordingly. See Section 5.1 for details.

The spectral semidiscrete-in-time problem obtained from (2.18) by substituting $L^2$ inner products and norms with LGL quadrature formulas reads:
for each $t \in (0, T)$ find $\boldsymbol{u}_N(t) \in [\mathbb{P}_N(\Omega)]^2$ such that $\boldsymbol{u}_N(t)_{|\Gamma_D} = \boldsymbol{\Phi}_N(t)$,

$$\begin{aligned}&\left(\rho \frac{\partial^2 \boldsymbol{u}_N}{\partial t^2}, \boldsymbol{v}_N\right)_N + a_N(\boldsymbol{u}_N, \boldsymbol{v}_N) + \langle -\boldsymbol{B}\boldsymbol{u}_N, \boldsymbol{v}_N\rangle_{\Gamma_{AB},N} \\ &\quad = (\boldsymbol{f}, \boldsymbol{v}_N)_N + \langle \boldsymbol{\Psi}, \boldsymbol{v}_N\rangle_{\Gamma_L,N} \quad \forall\, \boldsymbol{v}_N \in [\mathbb{P}_N^D(\Omega)]^2\end{aligned} \tag{4.5}$$

where $\mathbb{P}_N^D(\Omega) = \{\boldsymbol{v}_N \in \mathbb{P}_N(\Omega) : \boldsymbol{v}_{N_{|\Gamma_D}} = 0\}$ (we assume $\Gamma_D$ to coincide with one or more sides of $\Omega$).

Similarly, the spectral weak collocation approximation to (2.20) writes:
for each $t \in (0, T)$ find $\boldsymbol{u}_N(t) \in [\mathbb{P}_N(\Omega)]^2$ such that $\boldsymbol{u}_N(t)_{|\Gamma_D} = \boldsymbol{\Phi}_N(t)$,

$$\begin{aligned}&\left(\rho \frac{\partial^2 \boldsymbol{u}_N}{\partial t^2}, \boldsymbol{v}_N\right)_N + a_N(\boldsymbol{u}_N, \boldsymbol{v}_N) + \langle -\boldsymbol{B}\boldsymbol{u}_N, \boldsymbol{v}_N\rangle_{\Gamma_{AB},N} + \langle \boldsymbol{C}\boldsymbol{u}_N, \boldsymbol{v}_N\rangle_{\Gamma_{AB},N} \\ &\quad = (\boldsymbol{f}, \boldsymbol{v}_N)_N + \langle \boldsymbol{\Psi}, \boldsymbol{v}_N\rangle_{\Gamma_L,N} \quad \forall\, \boldsymbol{v}_N \in [\mathbb{P}_N^D(\Omega)]^2\end{aligned} \tag{4.6}$$

Then, for the case of ABC1 the stability estimate (3.12) obtained in Section 3 becomes

$$\|\boldsymbol{u}_N(T)\|_N^2 \le \int_0^T \|\boldsymbol{f}(s)\|_N^2 e^{C(t-s)}\, ds \tag{4.7}$$

whereas for ABC2 we obtain

$$
\begin{aligned}
\|\boldsymbol{u}_N(T)\|_N^2 \leq & \int_0^T \left(f, \frac{\partial \boldsymbol{u}_N}{\partial t}\right)_N \mathrm{d}t + \int_0^T \frac{\mu}{2} \left\langle \frac{\partial u_{1,N}}{\partial x_2} + \frac{\partial u_{2,N}}{\partial x_1}, \frac{\partial u_1,N}{\partial t} \right\rangle_{\Gamma_{AB},N} \mathrm{d}t \\
& + \int_0^T \left\langle \lambda \frac{\partial u_{1,N}}{\partial x_1} + (\lambda + \mu) \frac{\partial u_{2,N}}{\partial x_2}, \frac{\partial u_{2,N}}{\partial t} \right\rangle_{\Gamma_{AB},N} \mathrm{d}t \\
& - \int_0^T \left\langle \beta \frac{\partial^2 u_{1,N}}{\partial t\, \partial x_2}, \frac{\partial u_{1,N}}{\partial t} \right\rangle_{\Gamma_{AB},N} \mathrm{d}t - \int_0^T \left\langle \alpha \frac{\partial^2 u_{2,N}}{\partial t\, \partial x_2}, \frac{\partial u_{2,N}}{\partial t} \right\rangle_{\Gamma_{AB},N} \mathrm{d}t \\
& - (\alpha - \beta) \int_0^T \left[ \left( \frac{\partial u_{1,N}}{\partial t} \frac{\partial u_{2,N}}{\partial t} \right)(x_{1b}) - \left( \frac{\partial u_{1,N}}{\partial t} \frac{\partial u_{2,N}}{\partial t} \right)(x_{1a}) \right] \mathrm{d}t
\end{aligned}
\tag{4.8}
$$

Finally, the variational formulations (2.18) and (2.20), as well as the stability inequalities (3.12) and (3.29) holds true in the framework of *spectral element methods* too.

According to this method the original domain is partitioned into non-overlapping quadrilateral elements, each of them being mapped into a reference square. Within each quadrilateral element the solution is still a pair of algebraic polynomials of degree $\leq N$ in each variable. Therefore, the bilinear form $a_N(\cdot, \cdot)$, inner products $(\cdot, \cdot)_N$ and $\langle \cdot, \cdot \rangle_{\Gamma,N}$, and corresponding norms turn out to be the sums over all quadrilateral elements of the local LGL discrete ones (see next section).

Up to few changes of notations, the formulation of the semi-discrete spectral element problem can be stated and the stability estimates are obtained in a similar way.

## 5. Numerical results

In this section we present some numerical results in order to compare the performances of ABC2 with respect to the ones provided by ABC1. The spatial discretization is based on LGL collocation methods set in a variational form, whereas we use implicit backward finite differences for the time discretization.

### *5.1. Approximation by the spectral weak collocation method*

Here, we consider the spectral weak collocation method based on LGL points (e.g. [15–17]). Given a positive integer $N$ we introduce the LGL nodes in $[-1, 1]^2$ defined as the roots of the polynomial

$$
(1 - x_1^2)(1 - x_2^2) \frac{\partial L_N(x_1)}{\partial x_1} \frac{\partial L_N(x_2)}{\partial x_2}
$$

where $L_j(z)$ is the $j$th Legendre polynomial in $[-1, 1]$, and denote by

$$
X = \{\boldsymbol{x}_{km} = (x_{1k}, x_{2m}),\ 0 \leq k, m \leq N\} \tag{5.1}
$$

the corresponding nodes in $\Omega$.

We also define the $L^2$ discrete inner products, as well as the discrete bilinear form:

$$
(\boldsymbol{u}, \boldsymbol{v})_N = \sum_{i=1}^{2} (u_i, v_i)_N \equiv \sum_{i=1}^{2} \sum_{k,m=0}^{N} (u_i v_i)(\boldsymbol{x}_{km}) \omega_k^{x_1} \omega_m^{x_2} \tag{5.2}
$$

$$
a_N(\boldsymbol{u}, \boldsymbol{v}) \equiv \lambda (\operatorname{div} \boldsymbol{u}, \operatorname{div} \boldsymbol{v})_N + \mu \sum_{ij=1}^{2} (\epsilon_{ij}(\boldsymbol{u}), \epsilon_{ij}(\boldsymbol{v}))_N \tag{5.3}
$$

and

$$
\langle \boldsymbol{\Psi}, \boldsymbol{v} \rangle_{\Gamma,N} = \sum_{i=1}^{2} \langle \psi_i, v_i \rangle_{\Gamma,N} \equiv \sum_{i=1}^{2} \sum_{l} \Psi_i(P_l) v_i(P_l) \omega_l^{\xi} \tag{5.4}
$$

with $\Gamma = \Gamma_{\mathrm{L}}$ (or $\Gamma = \Gamma_{AB}$) where the sum runs over all nodes $\{P_l\} = \{\boldsymbol{x}_{km}\}$ lying on the portion of the boundary $\Gamma_{\mathrm{L}}$ (or $\Gamma_{AB}$) parallel to the $\xi$ axis.

In all cases the quantities $\omega_l^{\xi}$ are the discrete weights associated with the LGL quadrature formula in the $\xi$-direction.

We recall that

$$(u, v)_N = \int_{\Omega} uv \, dx_1 \, dx_2 \quad \text{if } uv \in \mathbb{P}_{2N-1}(\Omega) \tag{5.5}$$

We define

$$\|u\|_N = \sqrt{(u, u)_N} = \left( \sum_{i=1}^{2} \|u_i\|_N^2 \right)^{1/2}$$

$$\|\Psi\|_{\Gamma,N} = \sqrt{\langle \Psi, \Psi \rangle_{\Gamma,N}} = \left( \sum_{i=1}^{2} \|\Psi_i\|_{\Gamma,N}^2 \right)^{1/2}$$

The spectral weak collocation approximation of the elastodynamic problems with ABC1 or ABC2 has been reported before (see (4.5) and (4.6)).

We then apply a standard technique (e.g. [18–20]) consisting of choosing as $v_N$ the Lagrange basis functions associated with any collocation nodes of $X$. Using integration by parts rule and (5.5) it can be easily seen that problems (4.5) and (4.6) are equivalent to collocation problems. We refer to [3] for ABC1 (problem (2.18)) and report here the collocation formulation of ABC2 (problem (2.20)).

Precisely, we obtain

$$\boldsymbol{u}_N(P_k, t) = \boldsymbol{\Phi}_N(P_k, t) \quad \text{at } P_k \in \Gamma_{\mathrm{D}} \tag{5.6}$$

$$\left[ \rho \frac{\partial^2 u_{i,N}}{\partial t^2} + (A\boldsymbol{u}_N)_i - f_i \right] (\boldsymbol{x}_{km}, t) \omega_k^{x_1} \omega_m^{x_2} = 0 \quad \text{at } \boldsymbol{x}_{km} \in \Omega, \; i = 1, 2 \tag{5.7}$$

$$\omega_l^{\xi} [(C\boldsymbol{u}_N)_i - \omega_h^{\zeta} R_i](P_k, t) = 0 \quad \text{at } P_k \in \Gamma_{AB}, \; i = 1, 2 \tag{5.8}$$

$$\omega_l^{\xi} [(B\boldsymbol{u}_N)_i - \Psi_i - \omega_h^{\zeta} R_i](P_k, t) = 0 \quad \text{at } P_k \in \Gamma_{\mathrm{L}}, \; \mathrm{i} = 1, 2 \tag{5.9}$$

with $\xi = x_1$, $\zeta = x_2$ if $P_k = \boldsymbol{x}_{lh}$ lies on a horizontal side, whereas $\xi = x_2$, $\zeta = x_1$ if $P_k = \boldsymbol{x}_{hl}$ lies on vertical side and

$$R_i = f_i - \left[ \rho \frac{\partial^2 \boldsymbol{u}_N}{\partial t^2} + A\boldsymbol{u}_N \right]_i$$

is the equation residual.

From (5.8) it follows that the penalty residual method enforces the ABC2 weakly, as

$$(C\boldsymbol{u}_N)_i = \omega_h^{\zeta} R_i$$

at each LGL node on $\Gamma_{AB}$ and $\omega_h^{\zeta}$ is a one-dimensional LGL weight which vanishes as $N \to \infty$. As such, the treatment of ABC2 by the penalty residual method (4.6) has a strict analogy with the natural condition enforced for the prescribed loads (2.6) through Eq. (5.9).

We refer to Appendix A for the discussion of suitable strategies regarding the approximation of absorbing boundary conditions at vertex nodes.

### 5.2. The time advancing schemes

The semidiscrete continuous-in-time problem introduced in (5.6)–(5.9) can be considered as a system of second-order ordinary differential equations

$$\begin{cases} [D_2]\ddot{\boldsymbol{U}}(t) + [D_1]\dot{\boldsymbol{U}}(t) + [D_0]\boldsymbol{U}(t) = \boldsymbol{F}(t) \\ \boldsymbol{U}(0) = \boldsymbol{U}_0 \\ \dot{\boldsymbol{U}}(0) = \boldsymbol{U}_1 \end{cases} \tag{5.10}$$

where $[D_2]$ is a diagonal matrix, matrices $[D_1]$ and $[D_0]$ account, respectively, for first- and second-order partial derivatives with respect to the $x_1$ and $x_2$ variables, the vector $\boldsymbol{F}(t)$ is due to the contribution of external forces and loads, and $\boldsymbol{U}(t)$ is the vector of the displacement values $\boldsymbol{u}_N(x_{km}, t)$ at LGL nodes.

The full numerical treatment of the problem requires the time discretization of (5.10). An appropriate time advancing scheme should handle simultaneously the first- and second-time derivatives with respect to the $t$ variable, without compromising either of the global accuracy and the stability of the scheme. Several finite difference schemes have been tried for the acoustic and elastic wave equation, both explicit and implicit (e.g. [21, 3]).

Remind that for explicit methods the time step $\Delta t$ is subject to the stability condition

$$\Delta t \leqslant \frac{\kappa}{N^2} \tag{5.11}$$

for a suitable constant $\kappa$ depending on the wave propagation velocities and on the dimension of $\Omega$. Condition (5.11) shows that the stability restriction on $\Delta t$ becomes prohibitive for large values of $N$.

On the other hand, implicit methods turn out to be unconditionally stable regardless of the time step $\Delta t$. In particular, numerical results reported in [3] for ABC1 show that the allowable $\Delta t$ of the implicit scheme is about ten times larger than the one obtained by adopting an explicit advancing time scheme. Therefore, the computational burden due to the implicit scheme is repayed by larger admissible values of $\Delta t$ providing the same accuracy in the displacement Fourier spectrum of the explicit scheme.

An unconditionally stable method, which is second-order accurate with respect to $\Delta t$, is based on the B2–B2 scheme (*backward* 2nd order for $\partial^2/\partial t^2$ – *backward* 2nd order for $\partial/\partial t$):

$$\begin{aligned} \ddot{\boldsymbol{U}}(t_{k+1}) &\approx \frac{2\boldsymbol{U}_{k+1} - 5\boldsymbol{U}_k + 4\boldsymbol{U}_{k-1} - \boldsymbol{U}_{k-2}}{(\Delta t)^2} \\ \dot{\boldsymbol{U}}(t_{k+1}) &\approx \frac{3\boldsymbol{U}_{k+1} - 4\boldsymbol{U}_k + \boldsymbol{U}_{k-1}}{2\,\Delta t} \end{aligned} \tag{5.12}$$

Although each step requires the solution of a linear system, the matrix, being independent of $\Delta t$, can be factored once and for all at the beginning of the process. Several effective preconditioned iterative procedures based on the finite element method have also been proposed recently (e.g. [22,20,3]).

### *5.3. Numerical examples*

As a first example, we consider an elastic medium occupying the two-dimensional domain $\Omega = [-0.2, 0.2]^2$. The physical parameters are $\alpha = 6\sqrt{3}$, $\beta = 6$, $\rho = 1$. The numerical simulation is based on a LGL collocation grid corresponding to $N = 28$, giving a mesh of 841 points. Time marching is performed by the previously described B2–B2 scheme and adopting $\Delta t = 0.001$ for accuracy reasons. The source term $\boldsymbol{f}(t) = (f_1(t), f_2(t))$ in (2.3) is a spatial delta-function centered at $\boldsymbol{x} = (0, 0)$, as follows:

$$f_1(t) = \begin{cases} f_R(t) & \text{at } \boldsymbol{x} = (0,0) \\ 0 & \text{otherwise} \end{cases} \qquad f_2(t) = 0 \quad \text{in } \Omega$$

where

$$f_R(t) = [6\tilde{f}(t - t_0) - 4\tilde{f}^2(t - t_0)^3]\,e^{-\tilde{f}(t-t_0)^2}$$

$$\tilde{f} = (\pi f_{\max})^2 \qquad t_0 = 0.25 \qquad f_{\max} = 7.5$$

We set homogeneous initial conditions and either ABC1 or ABC2 on the whole boundary. In Figs. 2 and 3 we report the horizontal displacements of the body at two different receivers placed at the center $\boldsymbol{x} = (0, 0)$ (Fig. 2) and at the vertex $\boldsymbol{x} = (0.2, 0.2)$ (Fig. 3). Then, in Fig. 4 we report the strain energy

$$E(t) = \int_\Omega \left\{ \frac{\lambda}{2}\left(\frac{\partial u_1}{\partial x_1} + \frac{\partial u_2}{\partial x_2}\right)^2 + \frac{\mu}{2}\left[\left(\frac{\partial u_1}{\partial x_1}\right)^2 + \left(\frac{\partial u_2}{\partial x_2}\right)^2 + \left(\frac{\partial u_1}{\partial x_2} + \frac{\partial u_2}{\partial x_1}\right)^2\right]\right\} dx_1\, dx_2 \tag{5.13}$$

related to the elastic wave propagation. At each time level $t_k$ the quantity $E(t_k)$ is approximated through the LGL quadrature rule.

The energy pattern shown in Fig. 4 is due to the reduced size of the elastic medium: energy outcoming

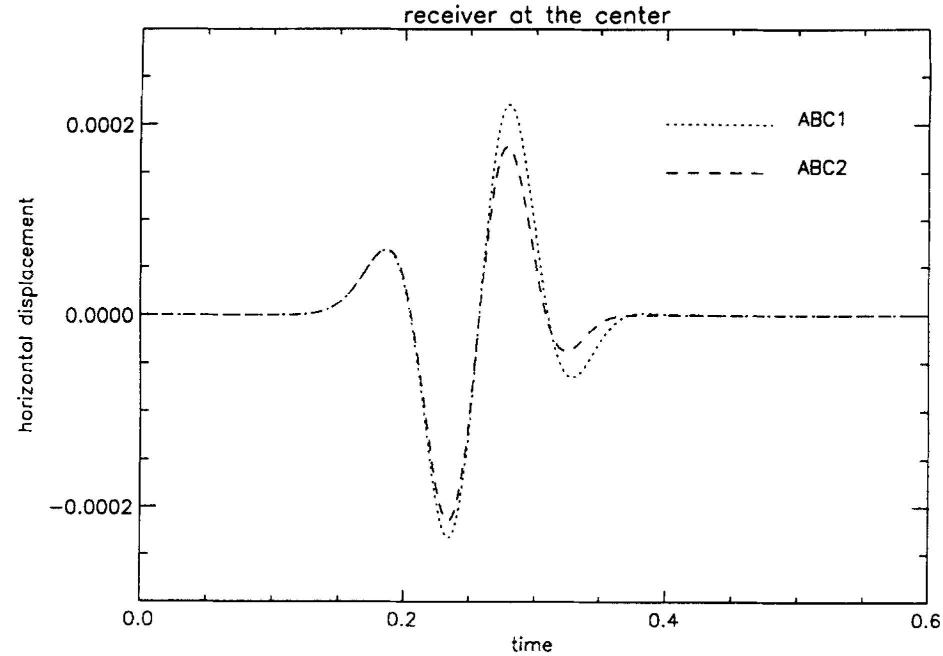


Fig. 2. Horizontal displacements of the body at the center of the square. Dashed and solid lines indicate, respectively, the results obtained from ABC1 and ABC2 analyses.

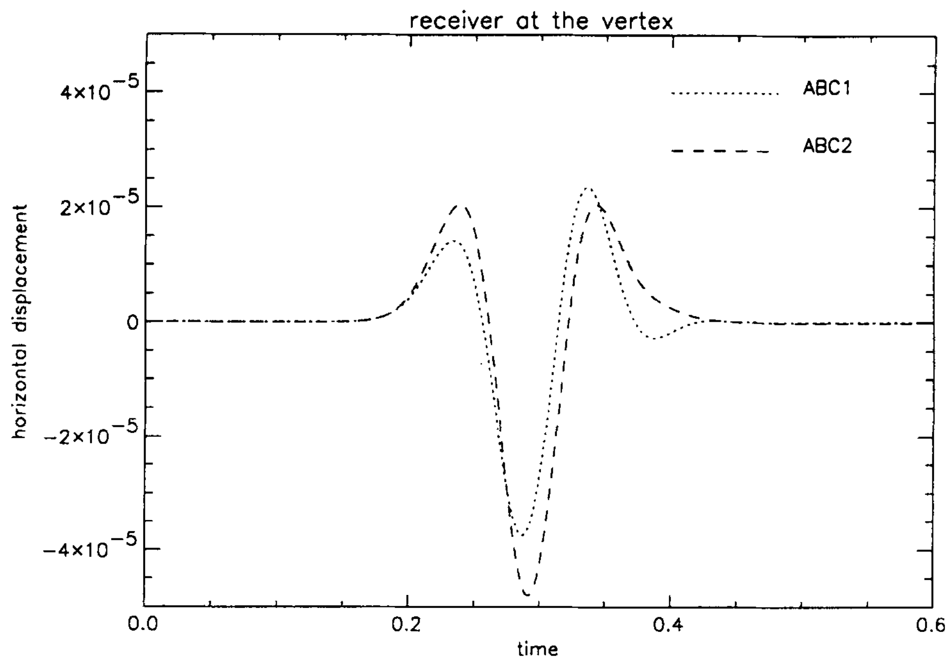


Fig. 3. Horizontal displacements of the body at the vertex of the square. Dashed and solid lines indicate, respectively, the results obtained from ABC1 and ABC2 analyses.

happens while energy provided by the source term is incoming. In Table 1 the $L_1$-norm of the energy is reported by adopting ABC1 and ABC2 conditions, respectively, for different values of $\Delta t$ and for $N = 28$.

As a second example we compare the Fourier spectral ratio (Fourier spectrum at output/Fourier spectrum at input) of the horizontal displacements of the body at the center of the square corresponding to ABC1 and ABC2 solutions with the one obtained by adopting an unbounded medium. In Table 2 $L_1$-norm, within the band

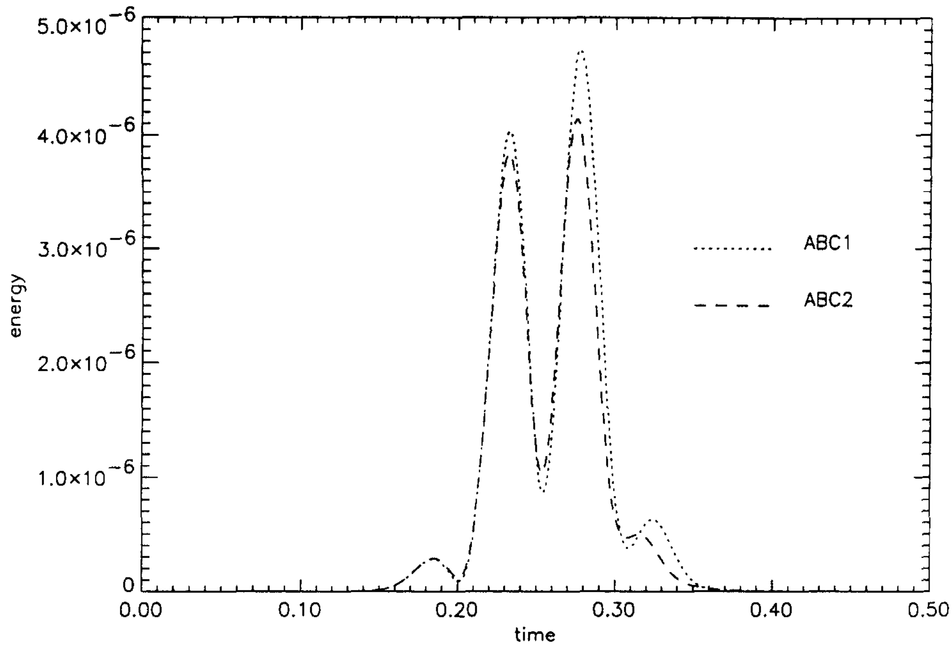


Fig. 4. Energy in the computational mesh. Dashed and solid lines indicate, respectively, the results obtained from ABC1 and ABC2 analyses.

Table 1

| $\Delta t$ | ABC1 | ABC2 |
|---|---|---|
| 0.001 | 2.73167 e − 7 | 2.48704 e − 7 |
| 0.005 | 2.71168 e − 7 | 2.49699 e − 7 |
| 0.01 | 2.48842 e − 7 | 2.35411 e − 7 |

Table 2

| $N$ | ABC1 | ABC2 |
|---|---|---|
| 20 | 20.34970 | 18.40492 |
| 24 | 20.50195 | 18.65718 |
| 28 | 20.64920 | 18.42195 |

frequency 0–20 Hz, of the relative error spectral ratio corresponding to ABC1 (or ABC2) conditions and an unbounded medium is reported with different $N$ values.

In the last example three receivers $A = (0.2, 0.2)$, $B = (0.2, 0.1)$ and $C = (0.2, 0.0)$ are considered. The same quantity of Table 2 is reported in Table 3 by using $\Delta t = 0.001$ and $N = 28$.

### 5.4. Stability

In this section we discuss the full numerical counterpart of the stability inequalities obtained in Section 4 for any semidiscrete continuous-in-time variational elastodynamic problem with ABC2. Apart from the choice of the discretization method for the spatial variables and derivatives, the integrals with respect to $t$ can be

Table 3

| receiver | ABC1 | ABC2 |
|---|---|---|
| A | 28.268 | 21.0317 |
| B | 24.667 | 15.6502 |
| C | 30.9410 | 23.7786 |

computed, for instance, through the composite trapezoidal formula. As a matter of fact, the discrete solution is available for each $t_k = k\,\Delta t$, $t_k \in [0, T]$ and the mentioned quadrature formula involves the values of the integrated function at the points $t_k$ only, whereas it does not require its value at the medium point of each discrete temporal subinterval. Then, the derivatives of the solution with respect to $t$ can be approximated through a finite difference scheme starting from the values of the solution at subsequent temporal instants. For instance, the backward 2nd order formula (5.12) for $\partial/\partial t$ can be adopted. The discretization of the spatial variables is here carried out through the LGL collocation methods. Therefore we refer in particular to the estimate (4.8).

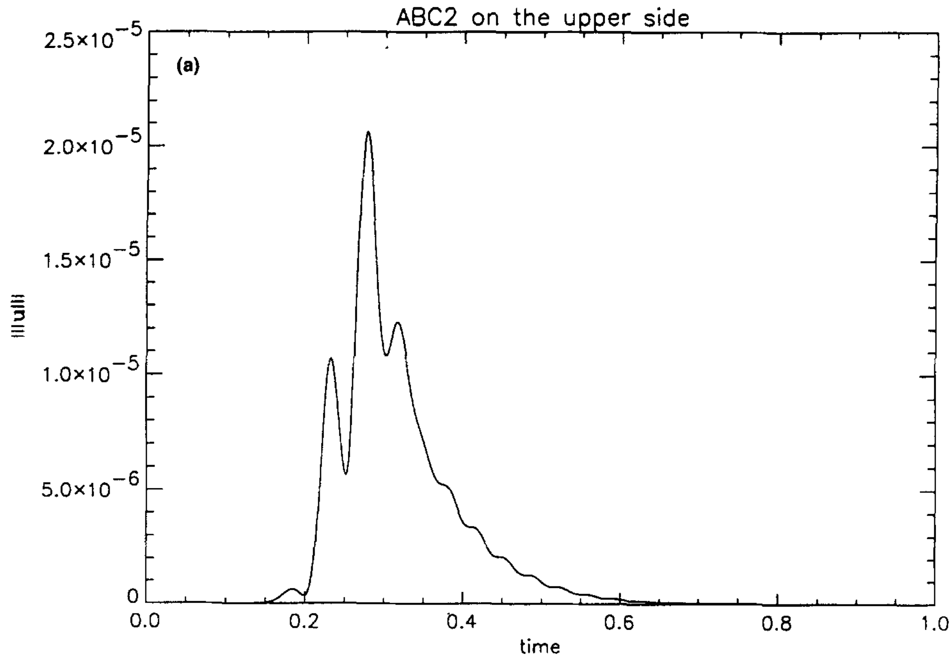


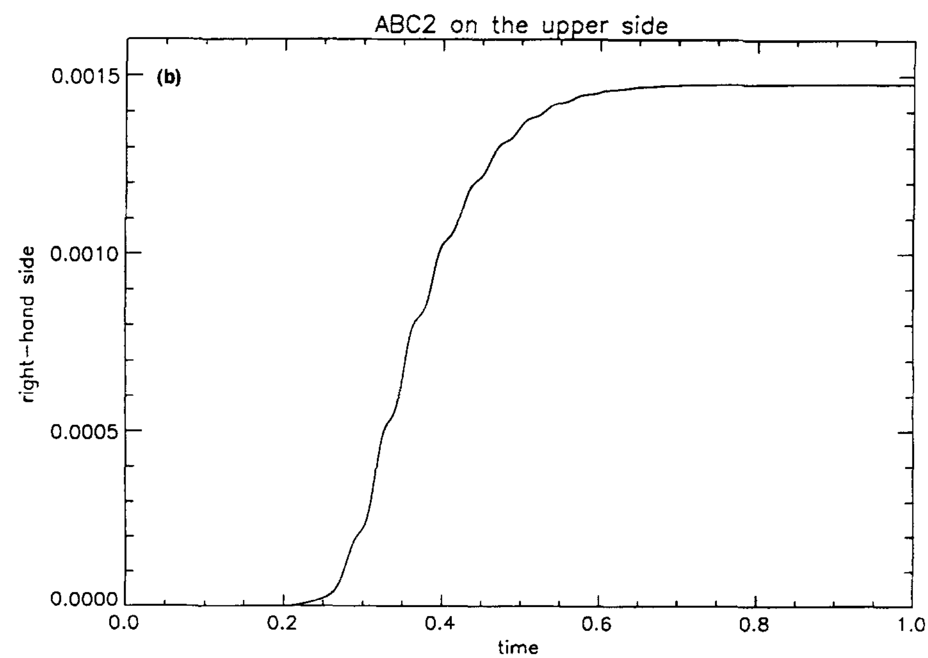


Fig. 5. Analysis of stability for the spectral collocation method. The boundary conditions are indicated in Fig. 1. Behaviour of the left-hand side $\|u_N\|_N$ (Fig. 5(a)) and the right-hand side (Fig. 5(b)) of the stability estimate (4.8) for increasing values of $t$.

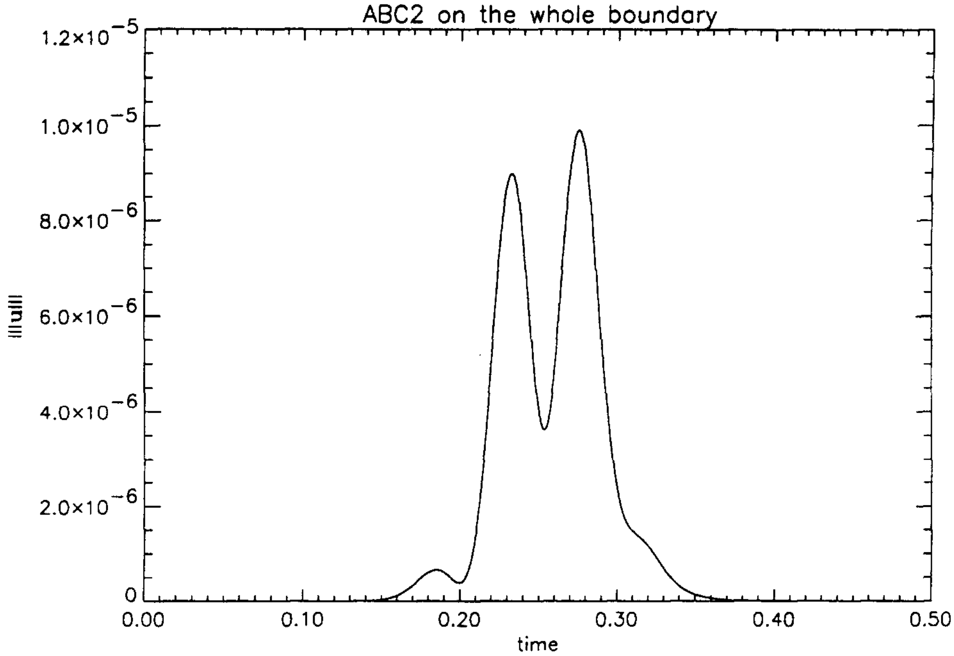


Fig. 6. $\|u_N\|_N$ for ABC2 on the whole boundary ($\Gamma_{AB} = \partial\Omega$).

For the same data as in Figs. 2–4 we compute both the left- and right-hand sides of (4.8) under the assumption of ABC2 on the upper horizontal side and homogeneous displacement boundary conditions on the remaining part of the boundary $\partial\Omega$ (see Fig. 1). In Fig. 5 we report the values of both left- and right-hand sides of (4.8), respectively. It should be noted that for $t$ growing the left-hand side, representing a suitable norm for the spectral solution, vanishes, whereas the right-hand side is bounded.

In the last example we consider the case of ABC2 on the whole boundary, i.e. $\Gamma_{AB} = \partial\Omega$ and in Fig. 6 we report the values of $\|u_N(t)\|_N$ for increasing values of $t$. Again, numerical results show that the discrete norm of the spectral solution vanishes for $t$ growing to infinity.

## 6. Conclusions

We have considered linear elasto-dynamic problems by implicit advancing time schemes and non-reflecting boundaries in the form of second-order paraxial conditions, that fit very conveniently into the variational formulation. The second-order paraxial condition is compared with the first-order one, and provides better results regarding the energy in the computational grid and the Fourier spectrum of the displacements.

## Acknowledgments

This research has been supported by 'Fondi MURST 40% Analisi Numerica e Computazionale' and 'Fondi di Ateneo' (ex 60%).

## Appendix A. Absorbing boundary conditions at corners

The treatment of domains with corners for the wave equations is very important from a practical point of view. If absorbing boundary conditions of order greater than or equal to 2 are implemented in a careless fashion, numerical calculations show that corners create instabilities. A brief discussion of some strategies at corners is reported in [8], both for acoustic and elastic wave equations, where it is proposed to use second-order absorbing boundary conditions away from the corner and first-order ones in the vicinity of the corner. A theoretical discussion guarantees stability of the scheme.

In finite difference calculations it is observed that it is needless to introduce a gradual transition region where the second-order approximate boundary condition is smoothly deformed to a first-order condition. Precisely, the higher order approximation can be used for all boundary mesh points except the corner and the two closest boundary grid points.

The more convenient strategy proposed in the finite difference approximation, both for acoustic and elastic wave equations, consists in rotating the first-order boundary condition so that it is exact for plane waves travelling in the direction of the bisector at the corner. Several other stable corner strategies having similar behavior regarding reflections were also proposed in [8]. A deep investigation of absorbing boundary conditions at corners, both from a mathematical and a numerical point of view, was carried out later in [23], where a new corner condition was presented along with different extensions. In particular, the authors analyzed a family of corner conditions, depending on a parameter, containing as a special case the one proposed previously in [8].

The construction of the corner condition is guided by two principles. On the one hand, the corner condition should preserve regularity of initial data. On the other hand, the expression of the corner condition should contain only first order spatial derivatives in a fixed direction. Following the guidelines of [8] and [23] we want to define suitable corner conditions for the approximation of the elastic wave equation by spectral collocation methods.

We remind that (e.g. [18,3]) the natural condition arising from the spectral variational scheme (3.6) neglecting the term involving the operator $C$ (2.17) and taking as test function the Lagrangian basis function associated with a corner (vertex) point $P_m$ reads

$$\left[\omega_i^{x_1}\omega_j^{x_2}\left(\rho\frac{\partial^2 \boldsymbol{u}_N}{\partial t^2}+A\boldsymbol{u}_N-\boldsymbol{f}\right)+\bar{k}_{x_2}\omega_i^{x_1}B_{x_2}\boldsymbol{u}_N+\bar{k}_{x_1}\omega_j^{x_2}B_{x_1}\boldsymbol{u}_N\right](P_m)$$
$$=[\bar{k}_{x_2}\omega_i^{x_1}\boldsymbol{\Psi}_{x_2}+\bar{k}_{x_1}\omega_j^{x_2}\boldsymbol{\Psi}_{x_1}](P_m) \tag{A.1}$$

where, according to the position of the vertex $P_m$, the indices $i$, $j$ and the integers $\bar{k}_{x_1}$ and $\bar{k}_{x_2}$ take the following values:

$$\begin{array}{llll} i=0,\ j=0\,, & \bar{k}_{x_1}=-1\,, & \bar{k}_{x_2}=-1\,, & \text{if } P_m=(x_{1a},x_{2a})\,,\\ i=N_i,\ j=0\,, & \bar{k}_{x_1}=+1\,, & \bar{k}_{x_2}=-1\,, & \text{if } P_m=(x_{1b},x_{2a})\,,\\ i=0,\ j=N_2\,, & \bar{k}_{x_1}=-1\,, & \bar{k}_{x_2}=+1\,, & \text{if } P_m=(x_{1a},x_{2b})\,,\\ i=N_1,\ j=N_2\,, & \bar{k}_{x_1}=+1\,, & \bar{k}_{x_2}=+1\,, & \text{if } P_m=(x_{1b},x_{2a})\,. \end{array} \tag{A.2}$$

Here, $\boldsymbol{\Psi}$ is a prescribed force at the boundary. Further, $B_{x_1}$ (respectively, $B_{x_2}$) denotes the restriction of the boundary operator $B$ to the vertical (respectively, horizontal) side merging into the vertex $P_m$.

For instance, at corner $(x_{1b}, x_{2b})$, we have

$$(B_{x_1}\boldsymbol{u}_N)_i=\sigma_{1i}(\boldsymbol{u}_N)\quad i=1,2 \tag{A.3}$$

$$(B_{x_2}\boldsymbol{u}_N)_i=\sigma_{2i}(\boldsymbol{u}_N)\quad i=1,2 \tag{A.4}$$

We propose to enforce at corner points the family of first-order absorbing boundary conditions (3.1), indicated here as ABC1, whose numerical implementation in a collocation fashion was carried out in [3]. For the seek of clarity, let us consider the corner condition at vertex $(x_{1b}, x_{2b})$. If we substitute ABC1 (3.1) into (A.1) we have

$$\left[\omega_{N_1}^{x_1}\omega_{N_2}^{x_2}\left(\rho\frac{\partial^2 u_{1,N}}{\partial t^2}+(A\boldsymbol{u}_N)_1-f_1\right)\right](x_{1b},x_{2b})$$
$$+\left[\omega_{N_1}^{x_1}\frac{\mu}{2}\left(\frac{1}{\beta}\frac{\partial u_{1,N}}{\partial t}+\frac{\partial u_{1,N}}{\partial x_2}\right)+\omega_{N_2}^{x_2}(\lambda+\mu)\left(\frac{1}{\beta}\frac{\partial u_{1,N}}{\partial t}+\frac{\partial u_{1,N}}{\partial x_1}\right)\right](x_{1b},x_{2b})=0 \tag{A.5}$$

$$\left[\omega_{N_1}^{x_1}\omega_{N_2}^{x_2}\left(\rho\frac{\partial^2 u_{2,N}}{\partial t^2}+(Au_N)_2-f_2\right)\right](x_{1b},x_{2b})$$
$$+\left[\omega_{N_1}^{x_1}(\lambda+\mu)\left(\frac{1}{\alpha}\frac{\partial u_{2,N}}{\partial t}+\frac{\partial u_{2,N}}{\partial x_2}\right)+\omega_{N_2}^{x_2}\frac{\mu}{2}\left(\frac{1}{\alpha}\frac{\partial u_{2,N}}{\partial t}+\frac{\partial u_{2,N}}{\partial x_1}\right)\right](x_{1b},x_{2b})=0 \qquad \text{(A.6)}$$

Equations at the remaining corners are set analogously.

## References


[1] Y. Maday and A. Patera, Spectral element methods for the incompressible Navier-Stokes equations, in: A.K. Noor and J.T. Oden, eds., State of the Art Surveys on Computational Mechanics (ASME, 1989) 71–143.

[2] R. Clayton and B. Engquist, Absorbing boundary conditions for acoustic and elastic wave equations, Bull. Seism. Soc. Am. 67(6) (1977) 1529–1540.

[3] E. Zampieri and A. Tagliani, Numerical approximation of elastic waves equations by implicit spectral methods, Comput. Methods Appl. Mech. Engrg. 144 (1997) 33-50.

[4] J. Carcione, Domain decomposition for waves propagation problems, J. Sci. Comput. 6 (1991) 453–472.

[5] E. Faccioli, A. Quarteroni and A. Tagliani, Spectral domain decomposition methods for the solution of elastic waves equations, Geophysics 61(4) (1996) 1160–1174.

[6] E. Priolo and G. Seriani, A numerical investigation of Chebychev spectral element method for acoustic waves propagation, in: R. Vichnevetsky, ed., Proc. 13th IMACS World Congress on Computational and Applied Mathematics (Criterion Press, 1991) 551–556.

[7] E. Tessmer, D. Kessler, K. Kosloff and A. Behle, Multidomain Chebyshev–Fourier method for the solution of the equations of motion of dynamic elasticity, J. Comput. Phys. 100 (1992) 355–363.

[8] B. Engquist and A. Majda, Absorbing boundary conditions for elastic wave calculations, Comm. Pure Appl. Math. 32 (1979) 313–357.

[9] P.A. Raviart and J.M. Thomas, Introduction a l'Analyse Numerique des Equations aux Derivees Partielles (Masson, Paris, 1983).

[10] J.L. Lions and E. Magenes, Nonhomogeneous Boundary Value Problems and Applications, Vol. 1 (Springer, Berlin, Heidelberg, New York, 1972).

[11] B. Engquist and A. Majda, Absorbing boundary conditions for numerical simulation of waves, Math. Comput. 31(139) (1977) 629–651.

[12] G. Bradfield, Use in industry of elasticity measurements in metals with the help of mechanical vibrations, N.P.L. Notes on Applied Science 30 (1964).

[13] R. Stacey, Improved transparent boundary formulations for the elastic wave equation, Bull. Seism. Soc. Am. 76 (1988) 2089–2097.

[14] R. Stacey, An explicit unstable mode in the Clayton and Engquist transparent boundary prescription, Bull. Seism. Soc. Am. 81 (1991) 694–698.

[15] C. Canuto, M.Y. Hussaini, A. Quarteroni and T.A. Zang, Spectral Methods in Fluid Dynamics (Springer Verlag, New York, 1988).

[16] P.J. Davis and P. Rabinowitz, Methods of Numerical Integration, 2nd edition (Academic Press, London, New York, 1984).

[17] A. Quarteroni and A. Valli, Numerical Approximation of Partial Differential Equations (Springer-Verlag, Berlin, 1994).

[18] A. Cividini, A. Quarteroni and E. Zampieri, Numerical solution of linear elastic problems by spectral collocation methods, Comput. Methods Appl. Mech. Engrg. 104 (1993) 49–76.

[19] A. Quarteroni and G. Sacchi Landriani, Domain decomposition preconditioners for the spectral collocation methods, J. Sci. Comput. 3 (1988) 45–76.

[20] E. Zampieri, On the condition number of some spectral collocation operators and their finite element preconditioning, J. Sci. Comput. 9 (1994) 419–443.

[21] F.Maggio and A. Quarteroni, Acoustic wave simulation by spectral methods, East–West J. Numer. Math. 2 (1994) 129–150.

[22] A. Quarteroni and E. Zampieri, Finite element preconditioning for Legendre spectral collocation approximations to elliptic equations and systems, SIAM J. Numer. Anal. 29 (1992) 917–936.

[23] A. Bamberger, P. Joly and J.E. Roberts, Second-order absorbing boundary conditions for the wave equation: a solution for the corner problem, SIAM J. Numer. Anal. 27 (1990) 323–352.